

# UC San Diego

## UC San Diego Electronic Theses and Dissertations

### Title

Myosin regulatory light chain phosphorylation and its role in active mechanics and force generation of the heart

### Permalink

<https://escholarship.org/uc/item/5x32s1qk>

### Author

Patel, Sejal

### Publication Date

2009

Peer reviewed|Thesis/dissertation

UNIVERSITY OF CALIFORNIA SAN DIEGO

Myosin Regulatory Light Chain Phosphorylation and its Role in Active Mechanics and  
Force Generation of the Heart

A Thesis submitted in partial satisfaction of the  
requirements for the degree Master of Science

in

Bioengineering

by

Sejal Patel

Committee in charge:

Professor Jeffrey Omens, Chair

Professor Andrew McCulloch

Professor James Covell

2009

Copyright

Sejal Patel, 2009

All rights reserved

The Thesis of Sejal Patel is approved, and it is acceptable in quality and form for publication on microfilm and electronically:

---

---

---

Chair

University of California San Diego

2009

To my parents CN & Aarti Patel,  
who left what they knew to provide me with the opportunities they never had, and to my  
family who provided me with the support, and encouragement which without, I would  
never be here today

## TABLE OF CONTENTS

Signature Page .....	iii
Dedication .....	iv
Table of Contents .....	v
List of Figures .....	vii
List of Tables .....	viii
Acknowledgments.....	ix
Abstract of the Thesis .....	xi
1. INTRODUCTION .....	1
1.1. Striated Muscle Contractile Function .....	1
1.2. Muscle Length-Dependent Activation.....	3
1.3. Cardiomyopathy and the Role of Regulatory Light Chain (RLC) Phosphorylation ...	6
1.4. Existing Models of Cardiac RLC Phosphorylation .....	9
1.5. A Novel Non-Phosphorylatable RLC Knock-in Model.....	12
1.6. Objectives .....	14
2. METHODS .....	16
2.1. Intact RV Papillary Muscle Isolation.....	16
2.2. Muscle Culture Chamber System Protocol .....	18
2.3. Data Analysis .....	20
2.4. Statistical Analysis.....	21
3. RESULTS. ....	22
3.1. Stretch Induced Immediate Force Response.....	22
3.2. Basal RLC Phosphorylation Effects On Baseline Force.....	26

3.3. Basal RLC Phosphorylation Potentiates Length-Dependent Force Generation .....	28
3.4. Basal RLC Phosphorylation & Diastolic Properties .....	32
4. DISCUSSION .....	33
5. CONCLUSIONS .....	41
REFERENCES .....	43

## LIST OF FIGURES

Figure 1.1: Regulation of Myosin RLC Phosphorylation in Striated Muscle.....	6
Figure 2.1: RV Papillary Muscle Tissue Culture Chamber System. ....	18
Figure 2.2: MLC2v and Wild-Type Stretched RV Papillary Muscles Mounted In Muscle Chamber.....	19
Figure 3.1: Active Stress Properties of Wild-Type Mice RV Papillary Muscles. ....	22
Figure 3.2: Normalized Maximum Rate of Force Development of Wild-Type Mice RV Papillary Muscles.....	24
Figure 3.3: Time To Peak of Normalized Force Data of Wild-Type Mice RV Papillary Muscles. ....	24
Figure 3.4: Active Force Generation Properties of Wild-type Mice RV Papillary Muscles Over Two Hours . ....	26
Figure 3.5: Peak Active Stress of MLC2v Knock-In and Wild-Type Mice RV Papillary Muscles .....	29
Figure 3.6: Stretch-Induced Increase in Active Stress of MLC2v and Wild-Type Mice .	30
Figure 3.7: Force Generation Increases Significantly in Response to Stretch in MLC2v Knock-In Mice.....	31
Figure 3.8: Peak Active Stress Data for Individual Wild-Type and MLC2v Knock-In Mice. ....	32



## LIST OF TABLES

Table 2.1: Chemical Concentrations of Cardiac Arrest Solution for Dissection And Chemical Composition of Diffusion Solution which Runs Through Tissue Culture Chamber for Experiment Duration. ....	16
Table 3.1: Systolic Properties of MLC2v Knock-In and Wild-Type Mice RV Papillary Muscles at Baseline (10% $L_{max}$ ) Stimulated at 1 Hz (n=5).....	27
Table 3.2: Systolic Properties of Wild-Type and MLC2v Knock-In Mice RV Papillary Muscles (N=7) at Baseline (Control, 10% $L_{max}$ ) and After Application of Isometric Load (Stretch, 90% $L_{max}$ ) Stimulated at 0.5 Hz .....	28

## ACKNOWLEDGEMENTS

This thesis represents a portion of one year of research within the Cardiac Mechanics Research Group in the Department of Bioengineering at the University of California San Diego. First, I would like to thank my advisors Dr. Jeffrey Omens and Dr. Andrew McCulloch for their guidance and patience. I learned so much from them both! Next, I would like to thank Dr. Covell for his constructive criticism, and thoughtful discussions. I would like to thank the members of the Medtronic team, especially Larry Mulligan, for their support, guidance and enthusiasm for my research as well as Walt Baxter for his mentorship.

I would also like to acknowledge Ju Chen and his research group. Without their support my research would have taken five times as long to finish. Farah Sheikh contributed equally to the RLC phosphorylation work published in this thesis. I feel honored to have had the opportunity to work with and learn from all of my mentors. Their support and guidance have been priceless.

I would like to thank Stuart Campbell, Joyce Chuang, Anna Raskin, Elliot Howard, and Darlene Hunt for their collaborations and input into my research study end-goals. Their enthusiasm in my work, which continued to motivate my interests in science, and their expertise helped me develop the experimental hypothesis and paradigms.

Lastly, I would like to thank all of my friends at CMRG, Bioengineering as well as my family and friends. I want to thank Nikhil for his patience, encouragement, and belief in me and Aboli for her constant support.

I would like to thank my dad for his continued interest in my work, and belief in scientific research. My mom, I especially appreciate for always believing in me and encouraging me to do my best, without her I would not be who I am today and have accomplished my goals. I want to thank my sister Minal for always genuinely supporting me and being an inspiration both intellectually and personally. As well as my brother Monil and sister Vanessa, for being both the support and the light in all of my endeavors.

## ABSTRACT OF THE THESIS

Myosin Regulatory Light Chain Phosphorylation and its Role in Active Mechanics and Force Generation of the Heart

by

Sejal Patel

Master of Science in Bioengineering

University of California San Diego, 2009

Professor Jeffrey Omens, Chair

Mutations that affect basal levels of myosin regulatory light chain (RLC) phosphorylation have been implicated in the development of familial hypertrophic cardiomyopathy. Regulatory light chains, one of the two light chain components of the myosin molecule, play a significant role in stabilizing the myosin lever arm during force transmission. While phosphorylation of RLCs by myosin light chain kinases have been implicated in modulating force development in cardiac muscle, their detailed mechanism

and precise role in cardiac function is not well understood as compared to their well-studied counterparts in skeletal muscle. In this study, the effects of RLC phosphorylation on cardiac force generation were assessed by comparing force generation results from wild type mice (~30% phosphorylated RLC) with those from a non-phosphorylatable RLC knock-in strain MLC2v (~0% phosphorylated RLC). Intact papillary muscles were isolated from mouse hearts, and placed within a tissue culture chamber system that enabled measurement of force within a physiologic environment, i.e. with controlled oxygen and superfusate delivery. This system enabled measurements of force generation before and after muscles were subject to an isometric stretch protocol (90%  $L_{max}$ ). RLC phosphorylation at baseline had no statistically significant effect on systolic force generation; however there was a profound difference in active stress between wild-type and MLC2v knock-in papillary muscles after isometric stretch. These results suggest that RLC phosphorylation potentiates the immediate force response to cardiac lengthening, i.e. the Frank Starling mechanism; therefore RLC phosphorylation may involve cross-bridge dynamics and compensatory protein phosphorylation mechanisms that are more complex than previously assumed.

## **1. INTRODUCTION**

### **1.1 STRIATED MUSCLE CONTRACTILE FUNCTION**

In cardiac muscle, contractile function is modulated by a complex mechanism involving thin and thick filament proteins. An action potential initiated by pacemaker cells in the sinoatrial node is propagated via gap junctions from non-contractile cardiac myocytes to contractile cells. The action potential triggers L-type calcium channels to release some calcium into the cell. This calcium release causes a positive feedback mechanism in which intracellular calcium ions trigger activation of ryanodine receptors in the sarcoplasmic reticulum membrane. This activation causes subsequent release of high levels of calcium into the cytosol [12,56].

Thereafter a complex mechanism involving the thin filament regulatory unit, including one troponin (Tn), one tropomyosin (Tm), and seven actin monomers, leads to force generation [12]. Tm is a double stranded helix that binds actin, and spans seven actin monomers. The current model of cross-bridge cycling involves calcium dependent transitions between three states, i.e. blocked, closed, and open, that lead to at least two distinct attached cross-bridge states, i.e. a weak-binding actin–myosin state (A-state) and a strong-binding actin–myosin state (R-state) [12,36].

In the absence of calcium with physiological MgATP concentrations and ionic strength, troponin I (TnI) binds tightly to actin, positioning Tm to block cross-bridge binding between actin and myosin (blocked state) [36]. When high levels of calcium are available in the cytosol, this causes calcium to bind to the N-terminus of troponin C (TnC). Tm moves toward the actin double helix groove (closed state). The calcium-TnC complex then has increased affinity for TnI, and TnC binds TnI; this allows Tm to move

positions on the actin filament. Once Tm re-positions itself, actin is able to weakly bind myosin (A state). The weakly bound actin-myosin cross-bridge then undergoes isomerization to form strong-binding, force-generating cross-bridges (R state). During this process, as the Tm is further embedded into the actin filament groove, the thin filament regulatory unit more readily moves into the open state. As more strong cross-bridges form, Tm is displaced further and further into the groove, exposing more actin sites that can bind myosin heads to form cross-bridges. This forms a positive feedback mechanism as adjacent thin filament regulatory filaments become sequentially activated and force generation is propagated [46]. This positive feedback mechanism is most pronounced in cardiac muscle where the binding of calcium to TnC and the conformation of TnC are further promoted by formation of strong cross-bridges [19,35,65].

In addition to the known mechanisms that induce contraction, other factors modulate the contractile function of cardiac tissue; for example cooperative interactions among proteins of the thin filament, thick-filament accessory proteins like C protein, sarcomere length of the muscle and phosphorylation of thick or thin-filament proteins like myosin light chains, myosin binding protein C and troponin I (TnI) may potentially modify cardiac force generation [40].

Phosphorylation of TnI at different sites, serine-43/45 or threonine-144, have differential effects on calcium sensitivity [51]. Phosphorylation of TnI at threonine-144 by PKC- $\beta$ II has been shown to increase calcium sensitivity in transgenic mice skinned myocytes [64] while phosphorylation of TnI at serine-43/45 depresses maximum tension and desensitizes the sarcomeres to  $\text{Ca}^{2+}$  in skinned mouse cardiac fiber bundles [2].

Interestingly, TnI phosphorylation overall has been shown to attenuate the length-dependent tension activation in cardiac muscle [26]. TnI has an inhibitory region that interacts with TnC to form a complex that can activate contraction by displacing the TnI inhibitory region from the interacting site of actin-Tm filament. However when TnI is phosphorylated, there is an interruption between the interaction of the inhibitory region of TnI and TnC and activation is decreased, which results in a rightward shift in the tension-pCa curve. When sarcomere lengthening occurs the distance between thick and thin filaments decreases; this in turn increases the probability of cross-bridge attachment to the thin filament and causes cooperative binding of neighboring cross-bridges leading to the development of larger tension. Phosphorylation of TnI decreases or attenuates the length-dependence tension activation (Frank-Starling mechanism) because when TnI is phosphorylated the inhibitory effect of TnI, as described above, decreases cross-bridge formation resulting in decreased effect of lengthening on tension activation [26].

Phosphorylation of myosin binding protein C (cMyBP-C) by calcium/calmodulin-dependent kinases (modulated by intracellular calcium), and by protein kinase A (modulated by  $\beta$ -adrenergic stimulation), determines the interaction of myosin with cMyBP-C [11]. The phosphorylation of cMyBP-C helps to pre-position the myosin head with respect to actin such that it facilitates cross-bridge attachment, and may even function in maintenance of thick filament spacing [11,19].

## **1.2 LENGTH-DEPENDENT ACTIVATION:**

Length-dependent changes in contractile function are physiologically significant in cardiology. The relationship between ventricular systolic function and end diastolic volume modulates cardiac function analogous to the modulation of muscle fiber



contractile function by lengthening (Frank-Starling mechanism) [12]. Existing studies are still attempting to identify the precise mechanism by which muscle fiber length modulates contractile force in striated muscle.

It is known that stretch associated reduction of lattice spacing leads to an increase in the number of myosin heads in close proximity to actin filaments; this increases the probability of actin and myosin forming strong binding interactions [13]. However, the mechanism underlying how lengthening results in increased force generation and calcium sensitivity is not fully understood [12].

Currently, length-dependent changes in force generation and calcium sensitivity are explained by two general themes that may be mutually inclusive [12]. One theme delineates that length-dependent changes are associated exclusively with a decrease in lattice spacing that directly leads to a closer proximity of actin and myosin heads. Subsequently, this leads to a higher probability of cross-bridge formation, and higher calcium sensitivity and maximum tension. However, myosin heads must be within a certain proximity of actin in order for stretch-induced reduction of lattice spacing to cause an increase in calcium sensitivity. If myosin heads are too far away from the actin molecule, then little or no change in force calcium sensitivity will occur [4]. Furthermore studies in skeletal muscle have shown that reduced lattice spacing due to stretch increases actin-myosin interaction by specifically increasing transition of cross-bridges and  $T_m$  dynamically from blocked to closed states [1,16].

Furthermore, studies have suggested that the large, elastic protein titin may play a role in coupling sarcomere length with a reduction in lattice spacing [14]. Stretch may

cause radial force to be transmitted through a strand of titin, and this transmission specifically results in a reduction of lattice spacing.

On the other hand, several studies have shown that increases in length have resulted in an increase in calcium sensitivity while osmotically-induced changes in lattice spacing did not. Consequently, there may be effects of length on actin-myosin kinetics that are independent of lattice spacing [27]. These effects of length may be attributed to a length sensing element that modulates actin-myosin interaction and increases calcium sensitivity and force generation.

Length-dependent activation may be exclusively caused by decreases in lattice spacing or may also be attributed to the effects of a length sensing element. Overall, lengthening controls the number of cross-bridges formed and therefore modulates calcium sensitivity and force generation. Furthermore, lengthening is influenced by factors such as protein phosphorylation, protein isoform expression, and the local physiochemical environment (temperature, pH, ionic strength, etc.) [12]. Changes in the Frank-Starling relationship associated with different conditions of protein phosphorylation have not been well studied in cardiac muscle models. In skeletal models, it has been shown that regulatory light chain (RLC phosphorylation) does not have a potentiating effect on force generation or calcium sensitivity in fibers with compressed lattice spacing [66]. Further study regarding the precise effect of basal RLC phosphorylation in length-dependent activation of cardiac muscle would shed light onto additional mechanisms that may potentiate or attenuate this critical response.

### 1.3 CARDIOMYOPATHY AND THE ROLE OF RLC PHOSPHORYLATION:

Cardiomyopathy is the leading cause of heart failure in the US and results in over 26,000 deaths annually, according to the American Heart Association 2005 US statistics. Systolic heart failure resulting from cardiomyopathy is the main cause of cardiovascular morbidity and mortality in both children and adults [5]. Following coronary artery disease, cardiomyopathy is the second most common cause of sudden death in the United States. One in about 500 people has familial hypertrophic cardiomyopathy (FHC), and 5 to 10% of people with FHC suffer fatal cardiac arrest [5].

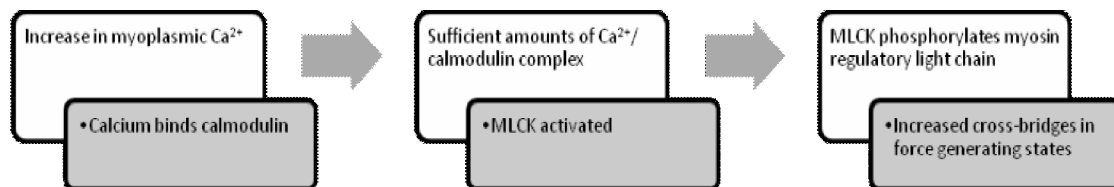


**Figure 1.1: Regulation of myosin RLC phosphorylation in striated muscle.**

Increases in intracellular calcium result in the formation of calcium bound calmodulin complexes that in turn activate myosin light chain kinases (MLCK). MLCKs then phosphorylate the myosin regulatory light chain and enhance systolic function.

Mutations in the ventricular myosin regulatory light chain (RLC), including those in close proximity to RLC phosphorylation sites, have been shown to cause familial hypertrophic cardiomyopathy; however the detailed mechanism and precise role of RLC phosphorylation in modulation of normal cardiac function is not well understood [28,60,61].

Myosin is an essential molecule of the contractile unit of striated muscle cells in vertebrates. The myosin hexamer is composed of two heavy chains and two light chains. Bound to the neck region of the heavy chain, myosin light chains, including an essential

and regulatory light chain, stabilize the myosin lever arm during force generation. RLC has been shown to be critical for modulating and maintaining normal cardiac function [6,7,18,22,28,30,41,47,50,55]. RLC phosphorylation is regulated by a calcium-calmodulin dependent mechanism [17]. Increases in intercellular calcium result in the formation of calcium-calmodulin complexes that activate myosin light chain kinases (MLCK); thereafter MLCKs phosphorylate myosin RLC (Figure 1.1). When calcium concentrations decrease due to calcium re-uptake into the sarcoplasmic reticulum, calcium dissociates and inactivates the holoenzyme complex resulting in calmodulin dissociating from MLCK. Myofibrillar protein phosphatases dephosphorylate the myosin regulatory light chain. PKC as well as Rho-activated kinase has also been implicated to effect phosphorylation of myosin RLC, however the nature and mechanism of these interactions remain unclear [51].

Basal RLC phosphorylation (~30% phosphorylated RLC [18]) plays a role in setting the kinetics of force development and calcium sensitivity in cardiac muscle [41]. In skinned myocardium, studies have shown that RLC phosphorylation enhances systolic function, i.e. increases tension and accelerates the “stretch activation” response [41,55].

The stretch activation response is implicated to play an important role in cardiac function [3,9,62] and is thought to play an intrinsic role in the oscillatory contraction of cardiac muscle [52]. Most dramatic in asynchronous insect flight muscles, stretch-activation enables continuous activation of the wing muscle to match aerodynamic loading [43]. The stretch activation response is important in modulation of cardiac muscle to a lesser degree, and may play a significant role in oscillatory power generation during systolic ejection. Stretch-activation is thought to enable cardiac muscle to match

increased mechanical loading, i.e. the steep Frank-Starling mechanism [55]. The basis of this hypothesis is that strong-binding cross-bridges cooperatively recruit additional strong-binding cross-bridges that enhance force generation in response to higher mechanical load. This cooperativity is independent of increasing concentrations of the main force-generation activator calcium. So overall, the response to stretch occurs in three phases: immediately after stretch there is an increase in force, force then decays to a minimum, and thereafter a redevelopment of force occurs, i.e. stretch-activation, due to this cross-bridge cooperativity [55].

Furthermore, while studies show that RLC phosphorylation increases calcium sensitivity of force [17,41,48], accelerates the rate of force development ( $k_{tr}$ ) in skinned skeletal muscle fibers [37,59], and increases maximally activated force in cardiac muscle, [41,55] some studies propose that cardiac RLC phosphorylation has no significant effect on maximally activated systolic force generation [39,58]. In addition, studies have proposed a transmural, spatial gradient of RLC phosphorylation across the ventricular wall and basal levels of RLC phosphorylation in the rat LV begin at ~20% RLC phosphorylation in the endocardium and rise to ~40% phosphorylation in the epicardium [6]. RLC phosphorylation gradients across the heart have been implicated in modulating systolic ejection and cardiac function.

Basal RLC phosphorylation has been proposed to increase calcium sensitivity and force generation via two underlying mechanisms. First, RLC phosphorylation causes the movement of the myosin head toward actin away from the thick filament backbone; this increases the probability of interaction between myosin and actin, and accelerates binding and transition of cross-bridges to force generating states [30,37,41,66]. In skeletal

muscle, it has been shown RLC phosphorylation causes the myosin head to lose its' nearly helical configuration and take-on a more disordered structure that enables the myosin head to be more mobile [66]. Second, RLC phosphorylation slows the rate of cross-bridge detachment, thereby decreasing the rate of cross-bridges returning to non-force generating states, prolonging the duty cycle, and enhancing contractile function [41]. This second mechanism is proposed as dominant because RLC phosphorylation results in distinctly slowed cycling kinetics [41].

Additionally, RLC is an EF-hand calcium-binding protein, like troponin and calmodulin. RLC contains one calcium binding EF-hand domain that enables it to bind calcium [55]. RLC phosphorylation has been shown to alter calcium binding properties of RLC in order to improve performance of a working muscle, or to restore function upon deficiencies caused by RLC mutations near its' calcium binding sites [60]. Mutations in RLC that potentially cause decreases in baseline and length-dependent immediate force responses, may be compensated for by phosphorylation of other contractile proteins as well, i.e. myosin binding protein C or TnI [50].

#### **1.4 EXISTING MODELS OF CARDIAC RLC PHOSPHORYLATION:**

Cardiac and skeletal muscle inherently differ in their mechanisms of force regulation. For example length-dependent changes in myofilament sensitivity are expected to play a prominent role in the beat-to-beat regulation only characteristic of cardiac muscle contraction, and cardiac TnC has only one calcium binding site while skeletal TnC has two which cause differences in activation [58]. Moreover, several studies have shown that cardiac and skeletal RLC lead to differing fiber kinetics and force generation properties [60]. While detailed mechanisms underlying RLC

phosphorylation have been well-studied in skeletal muscle models, the role of RLC phosphorylation is not fully understood in cardiac muscle.

Skinned muscle preparations are a model system for investigating calcium-dependent mechanisms. Due to free diffusional intracellular access, skinned muscles can easily model a precisely defined physiological state [53]. However, skinned preparations obscure the interactions between intercellular calcium transients and RLC calcium binding. Owing to the fact that RLC calcium binding sites and phosphorylation sites allosterically communicate, skinned preparations may potentially obscure RLC phosphorylation and its' effects on cardiac function. Additionally, the process of skinning a muscle results in fiber swelling that entails differences in lattice spacing, and overall may alter the sensitivity and cooperativity of myofilament  $\text{Ca}^{2+}$  activation [15]. Therefore, although the effects of RLC phosphorylation on force and stretch activation have been studied in skinned preparations of cardiac muscle [37,59,66], an intact muscle preparation, as employed in this study, may be a more physiologic model for studying RLC phosphorylation.

Extensions of the myocardial wall, papillary muscles are small muscles within the heart that anchor the heart valves, and contain 73.5% of cardiac muscle cells by volume [34]. Right ventricular papillary muscles have been widely used in functional studies of immediate load-induced cardiac mechanical phenomenon and long-term hypertrophy [34]. For numerous in vitro studies, a static load is applied to rabbit, mouse, ferrite, or rat papillary muscles and changes in force generation properties are examined at specific time periods following the application of the load [33]. Furthermore, twitch responses in papillary muscles and intact heart showed relatively similar results in steady contractile

activation [33]. Therefore in order to eliminate the complex dynamic architecture of the intact heart, isolated muscle or trabeculae preparations are ideal.

Intact mice papillary muscles or trabeculae have a distinct advantage over isolated cardiac myocytes because intercellular connections are maintained, and loaded contraction can be more clearly assessed [24]. Isolated papillary muscles will allow for controlled loading while maintaining samples at near-physiological conditions. In contrast to isolated stretched neonatal ventricular myocytes, the papillary muscle will allow for the continuous monitoring of contractile forces, twitch kinetics, and stress/strain relationship.

RV papillary muscles are thin (minor diameter:  $0.24 \pm 0.03$ ), unbranched, and numerous mouse hearts have papillary muscles that are suitable for isolation. Preparations of thin mouse ventricular trabeculae may also be applicable for this study, however not all mouse hearts have trabeculae suitable for isolation and culture. Trabeculae may be better suited for future studies in which specific chemicals, i.e. inhibitors or phosphatases, are administered to the muscle because in this case diffusion through the thinner surface of trabeculae is particularly beneficial.

Murine models are most applicable for this type of study because mice are small, prolific, and comprise a well characterized genome from which high-fidelity genetically modified models, like the MLC2v-S14/15A knock-in model, can be produced. A robust tool in scientific research, genetically modified mouse models can be employed to investigate the contribution of a specific protein in the length-dependent immediate force response of the heart, and in the overall mechanical properties of the heart. The tissue culture system employed in this experiment was developed specifically for wild-type and



genetically engineered mouse models to study cardiac mechanotransduction mechanisms [44].

Existing models of RLC phosphorylation modulate RLC phosphorylation levels via inhibition, i.e. with ML-9, or via de-phosphorylation, i.e. with BDM; these methods are not 100% specific for cardiac tissue MLCK or RLC respectively [18,41].

Furthermore, transgenic models of RLC phosphorylation have been used as well, but these models are not high fidelity.

### **1.5 A NOVEL NON-PHOSPHORYLABLE RLC KNOCK-IN MODEL**

Dr. Ju Chen has created a novel MLC2v-S14/15A knock-in model, the first high fidelity genetic model that results in effectively 0% RLC phosphorylation (unpublished data by Ju Chen). To develop this model, RLC genomic DNA was isolated from a mouse genomic DNA library and PCR based mutagenesis was used to generate a mutant gene encoding serine to alanine substitutions at positions 14 and 15, two-specific phosphorylation sites of RLC. The mutated DNA was electroporated into embryonic stem cells to replace the endogenous MLC2v gene and ES cells were microinjected into C57 mice blastocysts and transferred into pseudopregnant recipients. These recipients were repeatedly bred to obtain models with homozygous expression of mutated myosin RLC. Two-dimensional SDS-PAGE gels data on the double mutant mice, show that there is evidence of a low degree of phosphorylation at a possible additional phosphorylation site at serine-19 of RLC in the MLC2v knock-in model, however the amount of phosphorylation was low and insignificant.

MLC2v-S14/15A mice develop marked LV dilation and contractile dysfunction after 6 months of age (unpublished data from Dr. Ju Chen). This study employed

MLC2v knock-in mice at ages 6 to 8 weeks old, well before phenotypic changes were evident, to enable a more accurate investigation of the effects of basal myosin RLC phosphorylation. This study enabled the examination of the function of basal RLC phosphorylation via the employment of a novel high fidelity mouse knock-in model in which there was specific and complete elimination of cardiac RLC phosphorylation.

The interaction between protein phosphorylation and length-dependent activation is an area in need of further investigation [12]. While the interaction of phosphorylation of troponin I (TnI) with cardiac force-length dynamics have been studied, no published studies are available that explore the effects of RLC phosphorylation on cardiac lengthening (Frank-Starling mechanism) [12,26].

Employing a high-fidelity MLC2v-S14/15A knock-in model, this study novelly investigates the effects of basal cardiac RLC phosphorylation (~30% phosphorylated RLC [18]) on the force response to muscle lengthening in isolated, intact papillary muscles. This study demonstrates that RLC phosphorylation potentiates force generation in response to isometric load in intact mice papillary muscles; therefore non-phosphorylatable RLC knock-in mice (with effectively 0% RLC phosphorylation) display an attenuated immediate force response to isometric stretch. This attenuated immediate force response was manifested as a decrease in active stress. This study demonstrates that basal RLC phosphorylation potentiates the immediate force response to lengthening and affects the kinetics of force development in cardiac muscle.

## 1.6 OBJECTIVES

Mutations that affect basal levels of myosin regulatory light chain (RLC) phosphorylation have been implicated in the development of FHC in patients [60,61]. The detailed mechanism and precise role of RLC phosphorylation in modulation of normal cardiac function is not well understood. The objective of this thesis is to test the effects of RLC phosphorylation on force generation both at baseline and in response to load in intact mice papillary muscles; therefore non-phosphorylatable RLC knock-in mice (with effectively 0% RLC phosphorylation) were expected to show changes in baseline force generation properties and attenuated immediate force response to loading. Currently, scientific evidence has not demonstrated the contribution of RLC phosphorylation to lengthening induced immediate force generation, and no studies to-date have used a model with effectively 0% RLC phosphorylation. This study aims to corroborate that basal myosin RLC phosphorylation contributes to force development in cardiac muscle [6,7,8,18,22,28,41,55] as well as to find where RLC phosphorylation modulates the immediate force response to lengthening (Frank-Starling mechanism). Since mutations altering RLC phosphorylation levels lead to FHC, understanding the mechanism of RLC phosphorylation mechanism can potentially aid in targeted therapy development for FHC.

### *Specific Aims of Thesis:*

#### Aim 1. To confirm that stretch potentiates force generation in wild-type muscles

This study will test that in the current experimental paradigm, isometric stretch results in enhancement of systolic properties, i.e. an increase in active stress and rate of force generation as well as a decrease in time to peak, as expected.

Aim 2. To investigate the effects of basal RLC phosphorylation on force generation properties near slack length

This aim examined whether non-phosphorylatable RLC knock-ins display a decrease in systolic properties. A decrease is expected because the lack of RLC phosphorylation results in loss of movement of myosin head in closer proximity of actin (resulting in a decrease in rate of cross-bridges transitioning to force-generating states) and a more rapid rate of cross bridge detachment (resulting in an increase the rate of cross-bridges transitioning to non-force generating states) [41]. In addition, compensatory mechanisms, such as troponin I and myosin binding C protein phosphorylation may affect the force response in the MLC2v knock-in [11,19,28].

Aim 3. To investigate the effects of basal RLC phosphorylation on the immediate stretch response (1-2 minutes post application of stretch)

It is hypothesized that the systolic function of isometrically stretched wild-type mice will be increased owing to the combined effects of stretch and RLC phosphorylation potentiating force development. Stretch acts to place actin and myosin in closer proximity and RLC phosphorylation is expected to slow cross-bridge detachment, and leave cross-bridges in force-generating states for a longer time period. Systolic properties of MLC2v knock-ins will increase to a lesser extent due to only the effects of stretch [41]. In the MLC2v knock-in, complex compensatory mechanisms of contractile protein phosphorylation may be involved in this response as well [11,19,28].

## 2. METHODS

### 2.1 INTACT RV PAPILLARY MUSCLE ISOLATION:

All animal and experimental procedures were performed and approved according to the AAALAC animal guidelines and the guidelines of the University of California, San Diego Animal Care and Use Committee. Mice models were employed because mice are small, prolific and have a well characterized genome from which genetically modified models for phenotypes or disease states can be more easily produced. In order to eliminate the complex dynamic architecture of the intact heart, isolated papillary muscles were used. Isolated mice papillary muscles have a clear advantage over isolated cardiac myocytes because intercellular connections are maintained and loaded contraction can be assessed [24]. This study employed a mouse tissue culture chamber system (Figure 2.1) that allows for the continuous monitoring of contractile forces, twitch kinetics, and stress/strain relationship of isolated, adult, mouse cardiac papillary muscle preparations [44].

**Table 2.1: Chemical concentrations of cardiac arrest solution for dissection and chemical composition of diffusion solution which runs through tissue culture chamber for experiment duration.**

Chemical	NaCl	KCl	MgCl <sub>2</sub>	Na Acetate	Taurine	CaCl <sub>2</sub>	Glucose	Hepes	BDM
Cardiac Arrest Soln. (mM concentration)	137.2	<b>15.0</b>	1.2	2.8	10.0	<b>1.0</b>	10.0	10.0	<b>20.0</b>
Diffusion Soln. (mM concentration)	137.2	<b>5.0</b>	1.2	2.8	10.0	<b>2.0</b>	10.0	10.0	<b>N/A</b>

Owing to availability, initially wild-type (WT) NIH Swiss mice were used to test for the effects of stretch, i.e. Specific Aim 1 (n=5). With a sample size of n=7 for each group, WT C57/B6 or MLC2v-S14/15A (C57/B6 background) mice ages 6 to 8 weeks were used for experiments thereafter, i.e. Specific Aims 2 and 3. Non-phosphorylatable RLC knock-in strain MLC2v-S14/15A render effectively 0% RLC phosphorylation via the replacement of the endogenous MLC2v gene with a mutant gene encoding a substitution of serine to alanine at positions 14 and 15. At age 6 to 8 weeks, phenotype changes in the MLC2v-S14/15A knock-in model are not yet evident. MLC2v-S14/15A mice develop marked LV dilation and contractile dysfunction only after 6 months of age (unpublished data from Dr. Ju Chen). Wild-type mice had basal levels of approximately 30% RLC phosphorylation (unpublished Western Blot data from Dr, Ju Chen) [18].

Male C57 mice were anesthetized with Isoflurane. Cervical dislocation was performed, and following this the chest was opened. The heart was arrested by intracardiac injection of cardiac arrest solution (Table 2.1), containing high potassium (15mM), low calcium (1 mM) cardioplegic solution containing 20 mM of butanedione monoximen (BDM); after which the heart was quickly removed, and cannulated. Previously prepared, 10mM HEPES-buffered (pH=7.33) solution containing (mM): 137.2 NaCl, 15.0 KCl, 1.2 MgCl<sub>2</sub>, 2.8 Na Acetate, 10 Taurine, 1.0 CaCl<sub>2</sub>, 10.0 Glucose, and 20 BDM in equilibrium with 100% O<sub>2</sub> was then retrogradely perfused into the heart via the aorta. The blood was washed out and the right ventricle (RV) was opened. The RV papillary muscle was dissected from the interventricular septum taking care to leave a block of RV free wall tissue on one end and a portion of the tricuspid valve on the other.

Precautions were taken to avoid disturbance of the papillary muscle and to ensure that the chordae tendineae remained intact.

## 2.2 MUSCLE CULTURE CHAMBER SYSTEM PROTOCOL:

Next, the RV papillary muscle was mounted on a custom culture chamber with a bath (Figure 2.1) containing the HEPES-buffered cardiac arrest solution used in dissection [44]. The muscle is mounted between a stationary titanium hook, and a steel basket extension attached to the Harvard Apparatus force transducer (7224490) mounted onto an actuator-controlled (Newport CM-12CC), high precision bearing stage (Newport 460P-xyz). Muscles are continuously superfused with HEPES buffer solution at room temperature, and oxygen is delivered through an inlet tube into the chamber. The muscle was secured in the culture bath and thereafter the HEPES buffer solution was replaced by

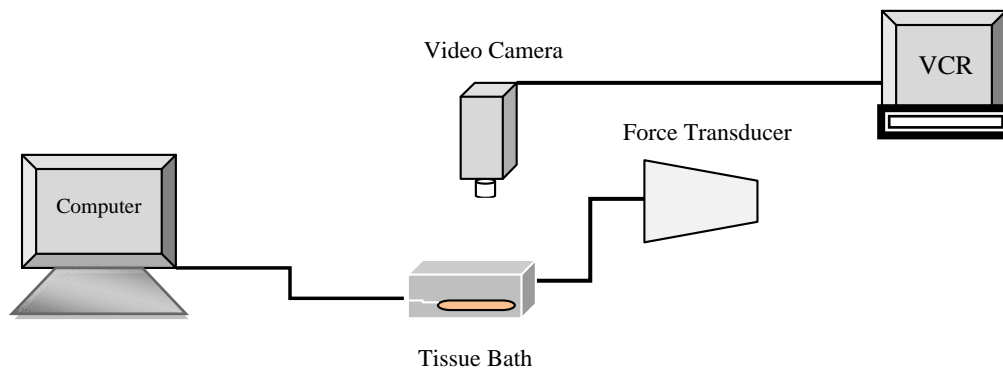


**Figure 2.1: RV papillary muscle tissue culture chamber system.**

Schematic of experimental set-up with an Isometric Harvard Apparatus force transducer (724490) to measure muscle force and a Newport CM-12CC actuator to adjust muscle length when papillary muscle is secured in the tissue bath between a basket and titanium hook.

the diffusion solution (Table 2.1) containing (mM): 137.2 NaCl, 5.0 KCl, 1.2 MgCl<sub>2</sub>, 2.8 Na Acetate, 10 Taurine, 2.0 CaCl<sub>2</sub>, 10 Glucose, and 10 Hepes in equilibrium with 100% O<sub>2</sub>. To maintain a constant supply of oxygen and nutrients to the muscle, a 100ml reservoir of oxygenated diffusion solution was continuously reperfused through the chamber at room temperature. After each experiment, both the cardiac arrest and diffusion solutions were sterilized via filtering and the tissue culture system was steam sterilized in preparation for subsequent experiments.

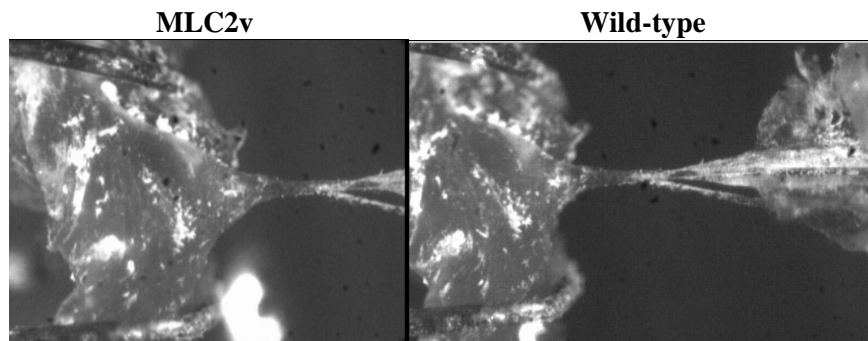


**Figure 2.2: MLC2v and wild-type stretched RV papillary muscles mounted in muscle chamber.** MLC2v and wild-type RV papillary muscle secured in the tissue bath between a basket and titanium hook. At age 6 to 8 weeks old, both wild-type and MLC2v papillary muscles are similar in appearance.

Muscles were stretched to 10%  $L_{max}$ , where  $L_{max}$  is defined as the length at which the muscle produces the greatest developed systolic tension. Muscles were field stimulated to contract between a platinum electrode, positioned within close proximity of the base of the muscle, and a titanium hook, near the top of the muscle. The muscle was equilibrated at 0.1 Hz for one hour. Once the forces stabilized, the stimulation frequency was increased to 0.5 Hz, and the muscle was stretched to 90%  $L_{max}$ ; control muscles were stretched to 10%  $L_{max}$  (Figure 2.2).



Length changes of the papillary muscle were detected with a linear voltage displacement transducer (Omega LD310-10). Right ventricular papillary muscles, marked with titanium dioxide particles (Figure 2.2), enabled recording of local muscle deformations by a CCD camera (COHU Inc.) (Figure 2.1). Forces were recorded during continuous stretching of the muscle up to  $L_{max}$  at 1 Hz. Afterwards, uniaxial muscle forces were recorded prior to and following the application of isometric stretch of the papillary muscle at 0.5 Hz. Signals representing length controller position, force, and stimulus voltage were digitized and recorded on a personal computer. Using video recording, muscle dimensions were acquired during experimentation. Following testing, the cross sectional area of each preparation was calculated, assuming that the muscle area was approximately elliptical in shape. This was used later to convert force measurements into muscle stress for final analysis of the data.

### **2.3 DATA ANALYSIS:**

From force and length raw data obtained from experiments, active developed stress, maximum rate of force development, and time to peak force were calculated as measurements of systolic function [32]. For every data point, five cycles of force data tracings were averaged over seven mice. For each cycle of force measurements, a polynomial curve of 5<sup>th</sup> order was fit to the data and then normalized by the peak force to obtain systolic parameters of force generation.

Active developed stress was calculated as the force at the base of the twitch minus the force at the peak of the contractile twitch divided by the area approximation of the muscle. The time to peak force was calculated employing the Windaq Waveform Browser software, which records real-time measurements as data was acquired. The

maximum rate of force development was determined via 1<sup>st</sup> order derivative approximation of the normalized, 5<sup>th</sup> order polynomial curve fit to the raw data.

The papillary muscles were marked with titanium markers prior to mounting into the culture chamber system, and deformation of the markers was recorded via a CCD video camera (COHU Inc.) (Figure 2.1). Local tissue stretch ratios were obtained by calculating the displacement of titanium dioxide markers along the vertical axis of the tissue. These stretch ratios were used to calculate the local Lagrangian surface strain measurements. A simple linear regression based model that correlates surface strain to sarcomere length was used as a reference to show that the surface strain values at  $L_{\max}$ , length at which maximal tension is produced, were well coordinated with sarcomere lengths of 2.2-2.3  $\mu\text{m}$  in published data [25,44].

#### **2.4 STATISTICAL ANALYSIS:**

The data was statistically evaluated using repeated measures ANOVA, and two-tailed un-paired (for WT vs. MLC2v-S14/15A) t-tests and two-tailed paired t-test (for 10%  $L_{\max}$ , control vs. 90%  $L_{\max}$ , stretch). This evaluated significance of differences to measured quantities at a P-value of 0.05. All data were expressed as mean +/- SEM, with n representing the total number of samples.

### 3. RESULTS

#### 3.1 STRETCH INDUCED IMMEDIATE FORCE RESPONSE

Wild-type NIH Swiss mice muscles were subject to stretch at 90%  $L_{max}$  and compared to control groups (n=5) in order to confirm that stretch had a significant effect on systolic function parameters peak active stress, maximum rate of force development and time to peak force. After the application of isometric loading or stretch, an initial increase in systolic force generation properties is expected as a result of length-dependent activation (the Frank-Starling mechanism) [12].

For a 30 minute time period, active properties were monitored to assess a significant effect of stretch on cardiac papillary tissue systolic function (Figure 3.1).

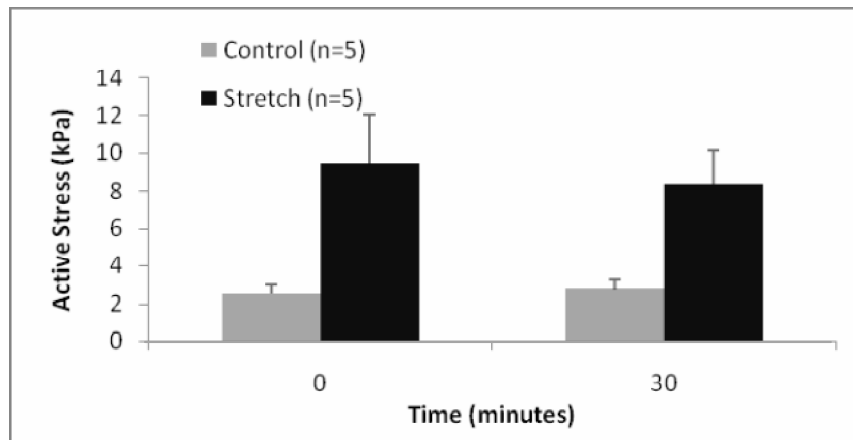


**Figure 3.1: Active stress properties of wild-type mice RV papillary muscles.**

Active stress in wild-type NIH Swiss RV papillary muscle (n=5) control group (10%  $L_{max}$ ) and stretch group (90%  $L_{max}$ ) during a 30 minute experimental paradigm at 1Hz. Data shows statistically significant changes in active stress at t=0 and t=30 minutes between control (10%  $L_{max}$ ) and stretch (90%  $L_{max}$ ) groups ( $P<0.05$ ). Data are mean  $\pm$  SEM.

Stretch had a statistically significant effect ( $P<0.05$ ) on peak active stress immediately (t=0) and even after 30 minutes of isometric stretch application (t=30).

There was on average an approximately  $7.0 \pm 2.2$  kPa increase in peak active stress immediately due to stretch; even up until 30 minutes after isometric stretch application there was an approximately  $5.6 \pm 0.4$  kPa increase in peak active stress. On average, this results in over a 3-fold increase in active stress immediately after stretch and an over 2-fold increase in active stress even after 30 minutes of stretch, taking fluctuations within the 30 minute time period in account. This immediate increase in active stress in mice papillary muscles due to isometric 90%  $L_{\max}$  stretch at 1 Hz stimulation frequency is comparable to published reports [57]. Specifically, wild-type muscles had an average active stress of  $9.45 \pm 2.6$  kPa comparable to those in previous studies with 0.5 Hz frequency and similar loading conditions both in mice and larger animal models [7,9,21,25,31,44,45]. Assuming an elliptical shape, the average calculated cross-sectional area of wild-type papillary muscle was  $0.032 \pm 0.009$  mm<sup>2</sup>; this was comparable to the average area of wild-type papillary muscles in published literature ( $0.04 \pm 0.01$  mm<sup>2</sup>) determined using similar assumptions [25]. Also  $L_{\max}$  in wild-type papillary muscles correlated relatively well with a sarcomere length of 2.2-2.3  $\mu\text{m}$ , which is characteristic of most myocardial papillary muscles and trabeculae in published literature [44]. Therefore observed changes in systolic properties were not associated with high variability in area or amounts of stretch between muscles.

Furthermore, the normalized maximum rate of force generation ( $dF/dt$ ) showed a statistically significant ( $P < 0.05$ ) increase with stretch at 90%  $L_{\max}$  (Figure 3.2). After the application of isometric stretch of 90%  $L_{\max}$ , there was approximately a 37% and 47% increase in the maximum rate of force development in muscles immediately after stretch ( $t=0$ ) and 30 minutes following application of isometric stretch, respectively. At  $t=0$ , the

values for normalized maximum rate of force development ( $6.4 \pm 0.5$ ) in non-stretch muscle were comparable to values in published literature [32].

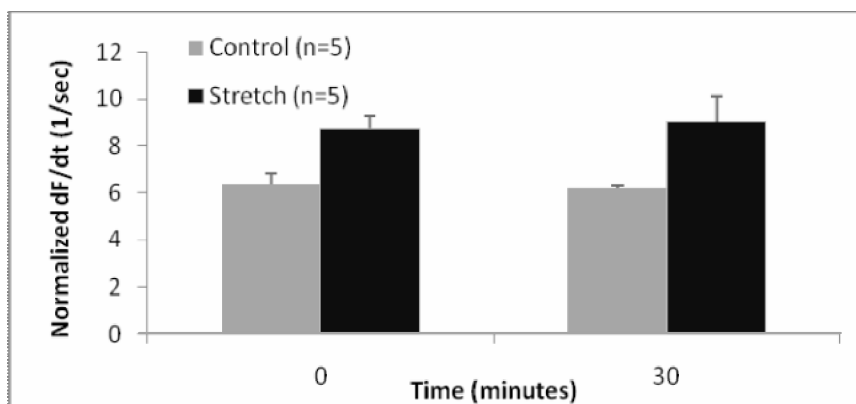


**Figure 3.2: Normalized maximum rate of force development of wild-type mice RV papillary muscles.**

Active stress in wild-type NIH Swiss RV papillary muscle (n=5) control group (10%  $L_{max}$ ) and stretch group (90%  $L_{max}$ ) during a 30 minute experimental paradigm at 1 Hz. Data shows statistically significant changes in normalized maximum rate of force development (normalized dF/dt) at t=0 and t=30 minutes between control (10%  $L_{max}$ ) and stretch (90%  $L_{max}$ ) groups ( $P < 0.05$ ). Data are mean  $\pm$  SEM.

Lastly, the systolic parameter of time to peak was measured immediately after the

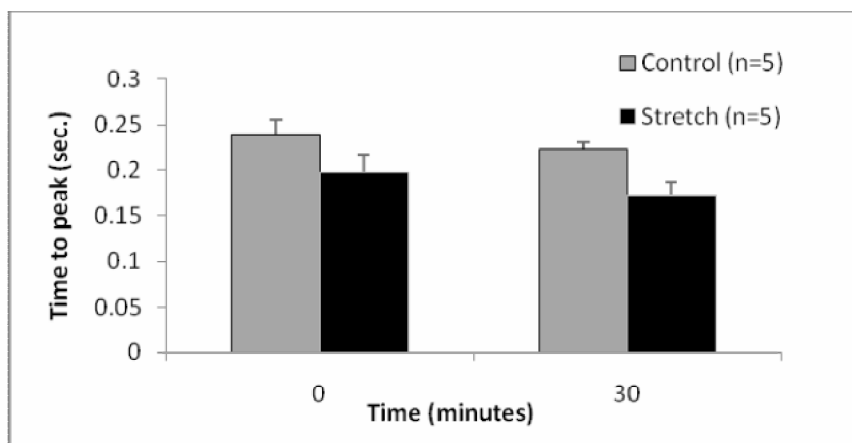


**Figure 3.3: Time to peak of normalized force data of wild-type mice RV papillary muscles.**

Time to peak force in wild-type NIH Swiss RV papillary muscle (n=5) control group (10%  $L_{max}$ ) and stretch group (90%  $L_{max}$ ) during a 30 minute experimental paradigm at 1 Hz. Data shows statistically significant changes in normalized time to peak at t=0 and t=30 minutes between control (10%  $L_{max}$ ) and stretch (90%  $L_{max}$ ) groups ( $P < 0.05$ ). Data are mean  $\pm$  SEM.

application of stretch at 90%  $L_{max}$  and after 30 minutes of load application at 90%  $L_{max}$  (Figure 3.3). Muscles stimulated at 0.5 Hz and stretched to 90%  $L_{max}$  had an average time to peak ( $0.2 \pm 0.04$  seconds) and average twitch duration comparable to previous studies [24,44]. Wild-type muscles showed on average a 17% decrease in time to peak as a result of immediate stretch. Both twitch duration, and time from activation to peak contraction, were also comparable to other studies [17, 37, 38, 39]

Isometric stretch or loading causes changes in the systolic function of isolated mice papillary muscles. The data indicate that immediate stretch causes an increase in active stress and maximum rate of force development in wild-type isolated mice papillary muscle. Furthermore, stretch induces an overall decrease in time to peak of papillary muscle contractions. These findings show that the system can carry out the protocol comparably to other studies. These results show that this preparation displays the well-studied Frank-Starling mechanism that lengthening or stretch results in immediate and significant increases in systolic force generation properties ( $P < 0.05$ ) [12].

Moreover, studies were conducted that showed that longer term stretch had effects on systolic function even after the immediate Frank-Starling mechanism. In these studies, muscles were held at 90%  $L_{max}$  for two hours and systolic force properties were measured. Results indicated that isometric stretch for two hours caused a decline in systolic function, i.e. active stress, and maximum rate of force generation ( $dF/dt_{max}$ ), over time which is comparable to data in published reports (Figure 3.4) [23,44]. While values at specific time points following stretch showed statistically significant changes in active properties, the overall temporal trend of active stress and  $dF/dt_{max}$  was not statistically significant. Further investigation is needed to understand why active

properties may change when subject to two hours of isometric stretch; these systolic function changes may be attributed to contractile protein cell signaling mechanisms that occur in response to constant isometric stretch within two hours.

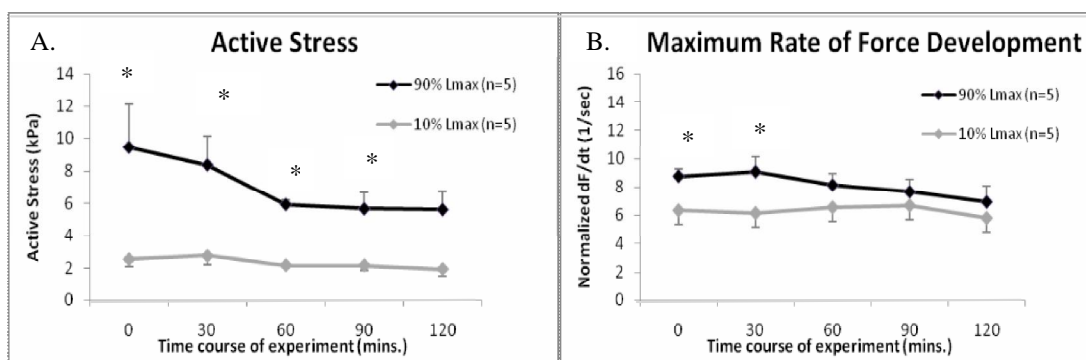


**Figure 3.4: Active force generation properties of wild-type mice RV papillary muscles over 2 hours.** Active force generation properties, i.e. active stress (A) and maximum rate of force generation (B) of wild-type RV papillary muscles (n=5) at baseline (control, 10% L<sub>max</sub>) and after application of isometric load (stretch, 90% L<sub>max</sub>) at 1 Hz. Values are expressed as mean  $\pm$ SEM. \* Indicates statistical significance (P<0.05).

### 3.2 BASAL RLC PHOSPHORYLATION EFFECTS ON BASELINE FORCE

To examine the hypothesis that basal RLC phosphorylation plays a role in setting the kinetics of force generation in cardiac muscle, the systolic properties of force generation, i.e. peak active stress, normalized dF/dt maximum, and time to peak force, were measured at baseline in wild-type and non-phosphorylatable MLC2v knock-in mice (n=7). Since the knock-in model effectively has 0% RLC phosphorylation (unpublished data by Ju Chen) and RLC phosphorylation is hypothesized to contribute to normal force development, it was expected that there would be a significant decrease in systolic function parameters.

Assuming an elliptical shape, the average calculated cross-section area of wild-type and knock-in papillary muscles was  $0.032 \pm 0.009 \text{ mm}^2$  and  $0.036 \pm 0.013 \text{ mm}^2$

respectively; these values were similar and comparable to the average area of wild-type papillary muscle ( $0.04 \pm 0.01 \text{ mm}^2$ ) using similar assumptions in the literature [25].

Therefore, observed changes in systolic properties were not associated with variability in area between the two models.

Results indicated that while there was a decrease peak active stress, normalized maximum  $dF/dt$ , and time to peak force, these decreases showed no statistically

**Table 3.1: Systolic properties of MLC2v knock-in and wild-type mice RV papillary muscles at baseline (10%  $L_{\max}$ ) stimulated at 1 Hz (n=5). Values are listed as mean  $\pm$ SEM.**

<b>Systolic Properties</b>	<b>Active Stress</b>	<b>dF/dt Maximum</b>	<b>Time to peak</b>
<b>Wild-type</b>	7.96 $\pm$ 1.60	9.51 $\pm$ 1.01	0.16 $\pm$ 0.015
<b>MLC2v</b>	6.29 $\pm$ 1.23	9.13 $\pm$ 0.28	0.18 $\pm$ 0.011

significant difference (Table 3.1). The active stress values at baseline for the wild-type and MLC2v knock-in mice were not significant with a power of 0.84, indicating confidence that there is no statistical difference between the values in the two datasets. The normalized maximum rate of force generation ( $dF/dt$  maximum) did not show a statistically significant difference between wild-type and MLC2v knock-in because the decrease between these values was relatively small, approximately 4%.

Furthermore, the maximum force increase in both the wild-type and MLC2v knock-in was determined in order to facilitate comparison to data from existing studies. Results indicated an approximately 5.5% increase in maximum force; however as in the



case for active stress, this increase in maximum force did not show statistical significance.

Overall, the data indicated no statistically significant changes in active properties between wild-type and MLC2v knock-in mice muscles near slack muscle length.

### 3.3 BASAL RLC PHOSPHORYLATION POTENTIATES LENGTH-DEPENDENT INCREASE IN FORCE GENERATION

To evaluate whether RLC phosphorylation does in fact potentiate the length-activated immediate force response, i.e. the Frank-Starling mechanism, systolic parameters peak active stress, maximum rate of force development and time to peak force were calculated for wild-type and MLC2v knock-in muscles (n=7) before (10%  $L_{max}$ )

**Table 3.2: Systolic properties of wild-type and MLC2v knock-in mice RV papillary muscles (n=7) at baseline (control, 10%  $L_{max}$ ) and after application of isometric load (stretch, 90%  $L_{max}$ ) stimulated at 0.5 Hz. Values are listed as averages  $\pm$ SEM.**

<b>Wild-type</b>	<b>Active Stress</b>	<b>dF/dt Maximum</b>	<b>Time to peak</b>
<b>Control (10% <math>L_{max}</math>)</b>	7.96 $\pm$ 1.60	9.51 $\pm$ 1.01	0.16 $\pm$ 0.015
<b>Stretch (90% <math>L_{max}</math>)</b>	15.23 $\pm$ 2.99	9.57 $\pm$ 0.96	0.18 $\pm$ 0.0203

<b>MLC2v</b>	<b>Active Stress</b>	<b>dF/dt Maximum</b>	<b>Time to peak</b>
<b>Control (10% <math>L_{max}</math>)</b>	6.29 $\pm$ 1.23	9.13 $\pm$ 0.28	0.18 $\pm$ 0.011
<b>Stretch (90% <math>L_{max}</math>)</b>	8.71 $\pm$ 1.3	9.49 $\pm$ 0.35	0.19 $\pm$ 0.0092

and after the application of isometric stretch (90%  $L_{max}$ ) (Table 3.2). Again, assuming an elliptical shape, the average calculated cross-section area of wild-type and knock-in

papillary muscles was  $0.032 \pm 0.009 \text{ mm}^2$  and  $0.036 \pm 0.013 \text{ mm}^2$  respectively; this was comparable to the average area of  $0.04 \pm 0.01 \text{ mm}^2$  determined of a wild-type papillary muscle using similar assumptions in published literature [25].  $L_{\max}$  in wild-type papillary muscles correlated well with a sarcomere length of 2.2-2.3  $\mu\text{m}$  characteristic of most myocardial papillary muscles and trabeculae in published literature [44]. Therefore, observed changes in systolic properties were not associated with high variability in area or amounts of stretch between wild-type and knock-in muscles.

Results indicate that there is a statistically significant difference ( $P < 0.05$ ) in the peak active stress values in knock-in mice and wild-type mice immediately after the application of isometric stretch (Figure 3.5). The approximately 2-fold increase in active stress due to stretch (90%  $L_{\max}$ ) at 0.5 Hz is comparable to data in previous studies

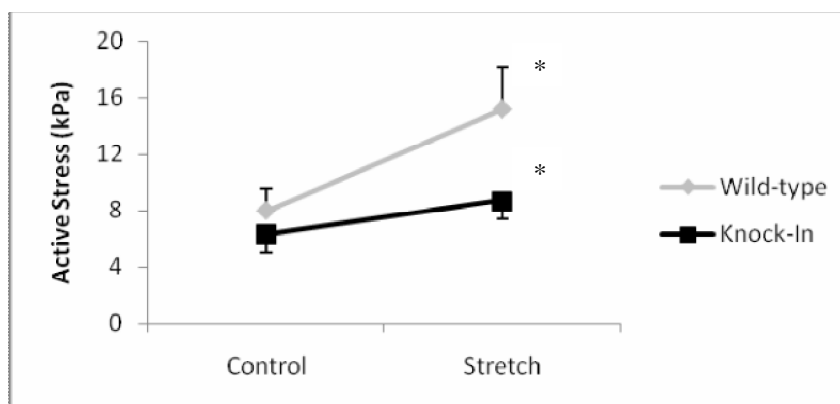


**Figure 3.5: Peak active stress of MLC2v knock-in and wild-type mice RV papillary muscles.**

Active force generation properties in non-phosphorylatable RLC knock-in strain (MLC2v-S14/15A) and wild-type RV papillary muscles ( $n=7$ ) at baseline (control, 10%  $L_{\max}$ ) and after application of isometric load (stretch, 90%  $L_{\max}$ ) at 0.5 Hz. Values are expressed as mean  $\pm$  SEM. \* Indicates statistical significance ( $P < 0.05$ ).

[8,38]. Peak active stress after the application of stretch in the MLC2v knock-in mouse is  $8.7 \pm 1.3 \text{ kPa}$  and in the wild-type mouse is  $15.2 \pm 2.9 \text{ kPa}$ , displaying an approximately

43% difference in peak active stress after stretch. Furthermore, the increase in peak active stress due to stretch is much greater in wild-type mice RV papillary preparations than in MLC2v knock-ins ( $P < 0.05$ ), as indicated by the slopes of the lines in Figure 3.5 and the values indicated in Figure 3.6. There was a 90% increase in peak active stress

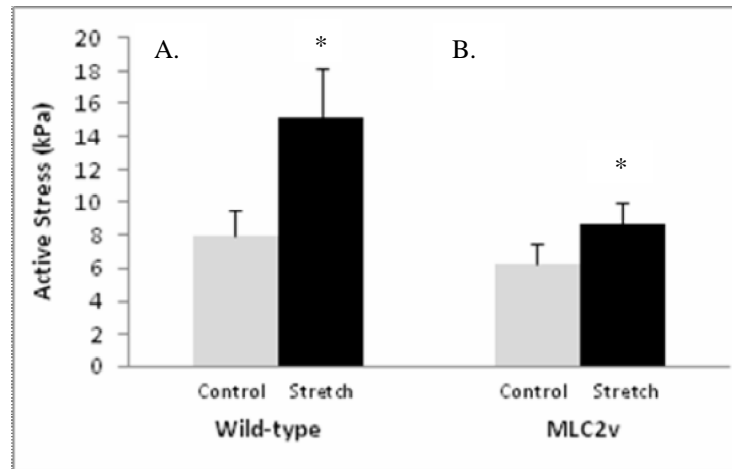


**Figure 3.6: Stretch-induced increase in active stress of MLC2v and wild-type mice.**

(A) Increase in peak active stress of wild-type mice RV papillary muscles ( $n=7$ ) from baseline at 10%  $L_{max}$  (control) to after application of isometric load of 90%  $L_{max}$  (stretch) at 0.5 Hz. (B) Increase in peak active stress of MLC2v knock-in mice RV papillary muscles ( $n=7$ ) from baseline at 10%  $L_{max}$  (control) to after application of isometric stretch of 90%  $L_{max}$  (stretch). Values are expressed as mean  $\pm$  SEM. \* Indicates statistical significance ( $P < 0.05$ ).

from control (10%  $L_{max}$ ) to stretch (90%  $L_{max}$ ) states in wild-type muscles ( $n=7$ ), while there was only a 38% increase in peak active stress in MLC2v knock-in mice from control to stretch states (Figure 3.7). Owing to the fact that non-phosphorylatable RLC (MLC2v) knock-in mice show a smaller increase in peak active stress due to stretch, this suggests that basal RLC phosphorylation potentiates the immediate force response to stretch.

Furthermore, not only on average but for each individual mouse the data indicates

that there is a greater increase in active stress due to stretch in wild-type muscle versus

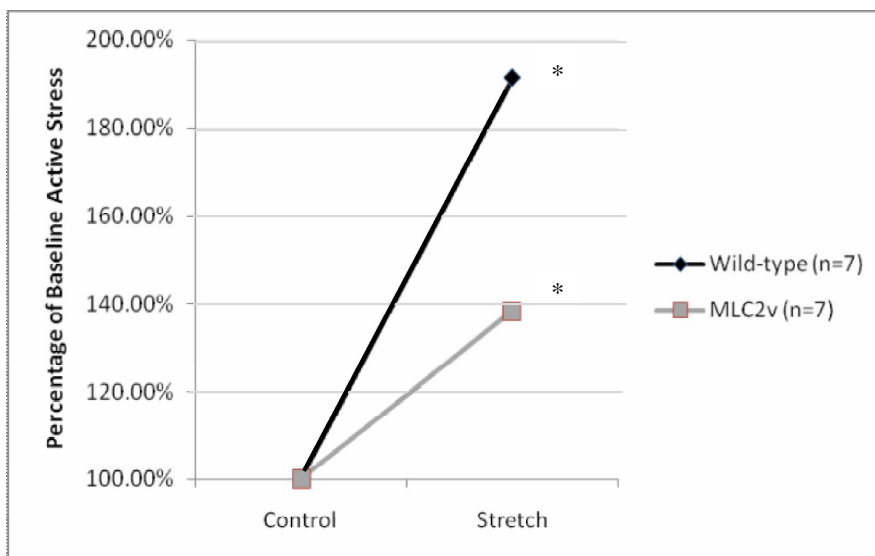


**Figure 3.7: Force generation increases significantly in response to stretch in MLC2v knock-in mice.** Active stress increases 90% in non-phosphorylatable RLC knock-in strain (MLC2v-S14/15A) while it increases only 38% in wild-type RV papillary muscles in response to stretch (90%  $L_{max}$ , n=7) at 0.5 Hz. Values are expressed as mean  $\pm$ SEM.

MLC2v knock-in mice (Figure 3.8). Data for four sample wild-type and MLC2v knock-in mice, displayed in Figure 3.8, clearly shows differences in slopes of the two datasets. Other systolic parameters, i.e. normalized maximum rate of force generation and the time to peak, did not show statistically significant differences between phenotypes in response to isometric stretch.

Furthermore, after 15 minutes of stretch application, there is a slight increase in active stress between the wild-type and MLC2v knock-in models, approximately 5%. However this change is not statistically significant and has low power values (less than 35%). This suggests that there may be a difference in the active stress that can be

detected with a larger sample size. These differences in active stress after 15 minutes of stretch may be attributed to a difference in the magnitude of the slow force response between wild-type and MLC2v knock-in mice. Since it has been proposed that RLC phosphorylation may contribute to the slow force response, this is an interesting area for further study [29].

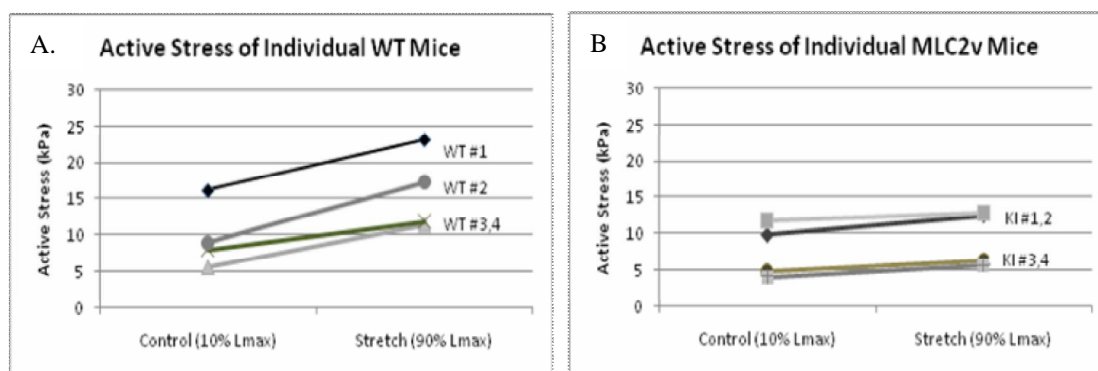


**Figure 3.8: Peak active stress data for individual wild-type and MLC2v knock-in mice.** Through comparisons of data from individual mice, it is apparent that peak active stress increases with a greater slope in response to stretch in wild-type (A) versus MLC2v knock-in (B) mice.

### 3.4 BASAL RLC PHOSPHORYLATION & DIASTOLIC PROPERTIES

Although the data showed no statistically significant changes of diastolic properties in MLC2v knock-in mice, i.e. end diastolic stress, maximum rate of relaxation, and time to 90% relaxation, the data indicated low power values (less than 40%) suggesting that differences in diastolic properties may be detectable at larger samples sizes. Diastolic properties after stretch in wild-type and MLC2v knock-in muscles showed no significant change. Further investigation of diastolic properties would be of interest to provide more insight into the interaction, if any, between RLC phosphorylation and diastolic properties of cardiac muscle.

#### 4. DISCUSSION

Previous studies have highlighted the relationship between protein phosphorylation and length-dependent activation as a significant area of study that is clearly in need of further investigation [12,18]. The present study is novel because no published literature has specifically explored the interaction between cardiac RLC phosphorylation and the length-tension relationship. Overall, the results indicate that RLC phosphorylation potentiates the immediate force response to stretch, i.e. the Frank-Starling mechanism. There was a statistically significant difference ( $P < 0.05$ ) in the peak active stress values in knock-in mice and wild-type mice immediately after the application of isometric stretch (Figure 3.5). Peak active stress after the application of stretch in the MLC2v knock-in mouse was  $8.7 \pm 1.3$  kPa and in the wild-type mouse was  $15.2 \pm 2.9$  kPa, displaying a 43% difference. Furthermore, there was a 90% increase in peak active stress from control (10%  $L_{max}$ ) to stretch (90%  $L_{max}$ ) states in wild-type muscles ( $n=7$ ), while there was only a 38% increase in peak active stress in MLC2v muscles from control (10%  $L_{max}$ ) to stretch (90%  $L_{max}$ ) states (Figure 3.7). This suggests that basal RLC phosphorylation plays a significant role in modulating the immediate force response to isometric stretch, i.e. the Frank Starling mechanism, in cardiac tissue.

The results also show that at slack length before samples were stretched, MLC2v and wild-type muscles did not have significantly different active stress or systolic properties. Peak active stress of wild-type mice was  $7.96 \pm 1.60$  kPa, while it was  $6.29 \pm 1.23$  kPa for MLC2v mice (Figure 3.6).

While some studies have shown that RLC phosphorylation increases calcium sensitivity of force [17,41,48], and increases maximally activated force in cardiac muscle

[41,55], other studies have indicated that RLC phosphorylation has no significant effect on maximal force or tension in rabbit and porcine skinned myocardium [39,58]. Olsson et al. [41] studied the effect of RLC phosphorylation on maximal force and calcium sensitivity in rat skinned trabeculae between experimental groups at ~7% phosphorylated RLC (post-BDM) and those at ~58% phosphorylated RLC (post-MLCK). The result of this study showed that maximum force increased by 5% and calcium sensitivity of force increased by 0.06pCa units. On the other hand, Morano et al. [39] showed that in porcine skinned myocardium, treatment with MLCK to increase RLC phosphorylation led to no statistically significant changes in maximal force. This study detected a 4.4% increase in maximal isometric force, however this increase did not show statistical significance. Similarly, the results of this study display a statistically insignificant 5.5% increase in maximal isometric force as a result of RLC phosphorylation in mice. Sweeney and Stull concluded that in rabbit myocardium RLC phosphorylation also had no significant effect on maximal force [58]. In addition, our studies showed that RLC phosphorylation had no significant effect on rise time or relaxation time, which concurs with published data in skinned trabeculae and other myocardial preparations from rat [41,47]. Lastly, changes in diastolic properties, i.e. end diastolic stress, rate of force relaxation, and time to 90% relaxation, were not statistically significant among experimental groups as well.

The differences in study results may be a result of experimental variables. Most studies described above used different fibers from those used in this study, and the majority of existing data on how RLC phosphorylation effects systolic function are from skinned preparations. As mentioned previously, skinned preparations have been shown to alter calcium binding of RLC and subsequently affect RLC phosphorylation because

RLC phosphorylation and calcium binding sites are shown to communicate allosterically. Also skinning a tissue sample can result in fiber swelling, which alters the lattice spacing within the tissue. In this study specifically, skinning can significantly alter the results because lattice spacing plays a key role in the lengthening response.

High sequence homology is apparent between amino acid sequences of cardiac RLC in different species [60]. However variability in data results may be attributed to differences in basal levels of RLC phosphorylation by species and ventricular spatial location of tissue [51,61]. While humans and large animals have four different isoforms of RLC, rodents only have two isoforms of RLC. The four different isoforms of RLC are two ventricular isoforms P1 and P2 and their phosphorylated counterparts P3 and P4 [51,61]. Therefore myosin RLC protein mechanisms, and levels as well as potency of basal RLC phosphorylation may differ between rodent and larger animal models.

The results of this study are significant and specifically can be explained by underlying mechanisms of cross-bridge dynamics as well as by compensatory protein phosphorylation signaling mechanisms in cardiac muscle. At baseline, when RLC phosphorylation is eliminated, there is a subsequent lack of RLC phosphorylation induced cross-bridge modifications and this results in decreased systolic force generation. RLC phosphorylation in cardiac muscle has been shown to cause myosin heads to move away from the thick filament backbone and come into closer proximity to actin as well as slow the rate of cross-bridge detachment; this results in an increase in the rate of cross-bridges forming and transitioning to force generating states, and causes a decrease in cross-bridges transitioning back to non-force generating states [41]. The net effect of this mechanism is to increase systolic force generation. Therefore, upon elimination of basal



RLC phosphorylation it is expected that there will be a subsequent decrease in rate of cross-bridges transitioning to force-generating states and an increase the rate of cross-bridges transitioning to non-force generating states; this causes an overall decrease in systolic function. However, this decrease in systolic function may have been compensated by phosphorylation of other contractile proteins, mainly TnI and cMyBP-C [11,28,51,61]. As mentioned previously phosphorylation of TnI at threonine-144 by PKC- $\beta$ II has been shown to increase calcium sensitivity in transgenic mice skinned myocytes [26]. Also phosphorylation of cMyBP-C by calcium/calmodulin-dependent kinases or by protein kinase A can pre-position the myosin head with respect to actin such that it facilitates cross-bridge attachment, and increases systolic function [11,19]. The initial decrease in systolic force may be compensated by the phosphorylation of TnI and/or cMyBP-C, which then would bring the net systolic force back up to normal levels. This would explain why in this study and in some reports, decreases or elimination of RLC phosphorylation did not result in significant changes in systolic properties [17,58].

After sarcomere lengthening, the underlying mechanisms of cross-bridge dynamics may be similar, however compensatory protein phosphorylation mechanisms may interact differently with cardiac lengthening associated cell signaling changes. First, upon elimination of basal RLC phosphorylation (~30% phosphorylated RLC [18]), it is hypothesized that there will still be a subsequent increase in the rate of cross bridge detachment resulting in decreased systolic function. Also, compensatory mechanisms such as phosphorylation of cMyBP-C and TnI may still be up-regulated in the knock-in. Although stretch may put actin and myosin in closer proximity, these compensatory mechanisms may significantly attenuate the length-dependent increase in systolic force.

cMyBP-C phosphorylation may contribute to increasing systolic force to baseline levels. However TnI phosphorylation overall has been shown to attenuate the length-dependent tension activation in cardiac muscle. Therefore, compensatory increases in TnI phosphorylation may contribute to the observed lack of length-dependent increase in force generation upon elimination of RLC phosphorylation [26]. Elimination of RLC phosphorylation will result in a decrease in systolic force attributed to lack of cross-bridge attachment enhancement, however compensatory mechanisms, i.e. cMyBP-C, will bring the systolic force back to baseline levels. Other compensatory mechanisms, i.e. TnI phosphorylation, may attenuate the force response to cardiac lengthening, resulting in the observed lack of significant force increase due to lengthening in the MLC2v model, and rather large difference in active stress after the immediate application of stretch between the wild-type and MLC2v mice.

Future studies can elucidate valuable information with respect to the current data, and can gain more in-depth information regarding remaining questions. In order to explore these possible compensatory protein signaling mechanisms and their interaction with cardiac lengthening, it would be important to investigate the levels and associated cross-bridge effects of phosphorylated TnI and MyBP-C after decreases in RLC phosphorylation level both at baseline and after stretch.

Also, developing a heterozygous knock-in model, with half phosphorylatable and non-phosphorylatable RLC, may be an insightful tool for exploring the effects of intermediate levels of phosphorylation as well. Nevertheless when developing these MLC2v knock-in models, it is important to keep in mind that substitutions of serine to alanine at RLC phosphorylation sites may entail additional effects both related and

unrelated to RLC phosphorylation. For example, this site specific mutation may effect the interaction between the calcium binding and phosphorylation sites of RLC, between the essential and regulatory light chains, between RLC and the heavy chain, between RLC and other contractile proteins, and the RLC protein conformation. The interactions between the regulatory light chain and heavy chain serve to stabilize the alpha-helical neck of the myosin head; therefore if this interaction is disturbed then cross-bridge cycling may be effected. Also, since calcium binding and phosphorylation sites on RLC may allosterically communicate, changes in RLC phosphorylation levels may affect RLC  $\text{Ca}^{2+}$  binding. This can lead to a disturbance of calcium homeostasis during muscle contraction and alterations in force generation, similar to those observed in other studies employing mice with mutations near the RLC phosphorylation site [60,61]. Furthermore, studies by Szczesna et al. [60,61] have demonstrated that mutations near the RLC phosphorylation site in mice cardiac muscle have lead to changes in alpha-helical content of the protein. This may also be the case for the mutation used in the present study; therefore MLC2v knock-in mutants may have an altered alpha-helical structure that may lead to sterical constraints of the molecule. This can potentially result in protein conformation changes or altered motion of the myosin lever arm. Precise repetitive motion of the myosin lever arm and tilt of the light chain domain are critical in enabling the myosin head to physically move away from the thick filament backbone towards the actin [61]. If mutations disturb this mechanism, then changes in cross-bridge cycling and force generation are entailed. Since charge is unchanged, the substitutions are conservative so that they cause minimal effects on RLC domain and protein interactions.

An alternative approach would be to conduct a paired study in which levels of RLC phosphorylation were increased and decreased in a single papillary muscle with MLCK inhibitors, i.e. ML-9, or molecules that dephosphorylate RLC, i.e. BDM or phosphatases. This type of experiment would be worthwhile because a paired model would reduce experimental variability among the control and experimental groups, and would facilitate comparison to existing results. It would be expected that decreasing levels of phosphorylation in the wild-type papillary muscles, via employment of molecular inhibitors or phosphatases, would render similar results to those of the knock-in and would align with the current data. This type of study would also elucidate if increased RLC phosphorylation correlates with an even higher increase in systolic force generation properties due to stretch. Trabeculae may be an ideal preparation for these types of experiments, not only because they comprise myofilaments that run in parallel enabling more uniform stretch, but also because they facilitate easier diffusion of oxygen and other molecules, i.e. inhibitors, through their comparatively thinner surface.

Although average levels of phosphorylation have been determined for wild-type and MLC2v mice models in this experiment, it would be advantageous to determine levels of phosphorylation of individual papillary muscle prior to experimentation and after stretch. This would minimize potential experimental variability due to differences levels of basal RLC phosphorylation by individual mice, spatial location of the tissue sample in the ventricular wall, and sarcomere length [6].

Moreover for future experimentation with papillary muscles, it may be relevant to probe the metabolic state of muscle, to ensure adequate diffusion of oxygen and nutrients

within the muscle. For example, nuclear magnetic resonance imaging or staining can be used to identify metabolites for signs of cell death or hypoxia.

Lastly, although surface strain at  $L_{\max}$  of papillary muscle tissue samples correlated relatively well with a sarcomere length of 2.2-2.3  $\mu\text{m}$ , in order to precisely standardize the stretch among the sample set, it may be useful to measure and control sarcomere length. Sarcomere-tension relationships are steeper than length-tension relationships, so therefore precise control and measurement of sarcomere length may prove insightful for future study. Sarcomere length can also serve as an experimental variant because stretch beyond  $L_{\max}$  can result in the middle portion generating a length-dependent increase in active force while the ends generate lower active force due to overstretch. This can cause non-homogenous stretch protocols and variability within the dataset. For this experiment, the muscle chamber attachment system was designed such that it minimized damage to the ends of the muscle to reduce variability among samples and promote standardized results for each experiment.

## 5. CONCLUSIONS

The results of this study provide novel insights into the contribution of basal RLC phosphorylation to cardiac force generation and the interaction of RLC phosphorylation with cardiac lengthening. We have found that while MLC2v knock-in mice with effectively 0% RLC phosphorylation showed similar baseline force generation properties, they had attenuated force responses to cardiac lengthening. These changes were not associated with significant differences in post-stretch sarcomere length or muscle area. Therefore basal RLC phosphorylation may potentiate the immediate force response to stretch, i.e. the Frank Starling mechanism. The baseline force generation results for MLC2v mice correlated well with data from skinned myocardial preparation in rabbit and porcine with reduced RLC phosphorylation levels [39,58].

While elimination of RLC phosphorylation can lead to cross-bridge modifications that result in decreased systolic function, compensatory phosphorylation of other contractile proteins, mainly TnI and cMyBP-C, may bring systolic force back to normal levels [11,19,20,26,28]. This would explain why no significant differences were observed in baseline active stress between wild-type and MLC2v mice. Also after cardiac lengthening, elimination of RLC phosphorylation resulted in a decrease in systolic force attributed to a lack of RLC induced cross-bridge enhancement; however compensatory mechanisms, i.e. cMyBP-C phosphorylation, may bring the systolic force back to baseline levels. It is possible that an additional compensatory mechanism may come into play as well, i.e. TnI phosphorylation, and this mechanism has been shown to attenuate the force response to cardiac lengthening [26]. If compensatory increases in TnI phosphorylation did occur, this may explain the lack of steep increase in active stress

due to lengthening in the MLC2v model, and rather large difference in active stress between the wild-type and MLC2v mice after stretch.

These results add new insights into the molecular players and potential complex signaling events that contribute to baseline and length-dependent force generation. While MLC2v mice have a mutant gene encoding serine to alanine substitutions at two specific RLC phosphorylation sites, it is important to keep in mind that these substitutions may have additional effects on protein conformation, allosteric site interactions and protein-protein interactions.

This study lays a foundation for future studies on RLC phosphorylation and its contribution to contractile function of the heart. Future directions of study may include employing a paired model, in which levels of RLC phosphorylation are increased and decreased in the same mouse, to compare effects of various levels of RLC phosphorylation on the immediate force response to stretch. Also future studies may enable a better understanding of the complex interaction of compensatory protein phosphorylation mechanisms and cross-bridge dynamics that may come into play upon elimination of basal RLC phosphorylation. Overall these studies have the potential to pave the way for future therapies targeting diseases such as familial hypertrophic cardiomyopathy [28,60,61].

## REFERENCES

1. Brenner B, Yu LC & Podolsky RJ (1984) X-ray diffraction evidence for cross-bridge formation in relaxed muscle fibers at various ionic strengths. *Biophys J* 46: 299–306.
2. Burkart-Dagger EM, et al. (2003) Phosphorylation or Glutamic Acid Substitution at Protein Kinase C Sites on Cardiac Troponin I Differentially Depress Myofilament Tension and Shortening Velocity. *J. Biol. Chem.* 278 (13): 11265-11272.
3. Campbell KB, & Chandra M. (2006) Functions of Stretch Activation in Heart Muscle. *J. Gen. Physiol.* 127:89–94.
4. Cazorla O, Wu Y, Irving TC & Granzier H (2001) Titin-based modulation of calcium sensitivity of active tension in mouse skinned cardiac myocytes. *Circ Res* 88: 1028–1035.
5. Daughenbaugh, LA (2007) Cardiomyopathy: An Overview. *Journal for Nurse Practitioners.* 3(4):248-258.
6. Davis JS, Hassanzadeh S, Winitsky S, et al. (2001) The overall pattern of cardiac contraction depends on a spatial gradient of myosin regulatory light chain phosphorylation. *Cell.* 107:631-641.
7. Dias, FA et al.(2006) The effect of myosin regulatory light chain phosphorylation on the frequency-dependent regulation of cardiac function. *J Mol Cell Cardiol.* (2):330-339.
8. Edman, KAP, et al. (2005) Contractile properties of mouse single muscle fibers, a comparison with amphibian muscle fibers. *Journal of Experimental Biology* 208, 1905-1913.
9. Epstein ND, & Davis JS. (2003) Sensing stretch is fundamental. *Cell.* 112:147–150.
10. Epstein, ND, & Davis JS (2006) When is a fly in the ointment a solution and not a problem? *Circ. Res.* 98:1110–1112.
11. Flashman E, Redwood C, Moolman-Smook J, & Watkins H (2004) Cardiac Myosin Binding Protein C: Its Role in Physiology and Disease. *Circulation Research* 94:1279.
12. Fuchs F, & Martyn DA (2005) Length-dependent Ca<sup>2+</sup> activation in cardiac muscle: some remaining questions. *J. Muscle Res. Cell Motil.* 26:199–212.
13. Fuchs F & Smith SH (2001) Calcium, cross-bridges, and the Frank–Starling relationship. *News Physiol Sci* 16: 5–10.



14. Fukuda N, Wu Y, Irving TC & Granzier H (2003) Titin isoform variance and length dependence of activation in skinned bovine cardiac muscle. *J Physiol* 553: 147–154.
15. Godt RE, & Maughan DW (1977) Swelling of skinned muscle fibers of the frog. Experimental observations. *Biophys J* 19:103–116
16. Head JG, Ritchie MD & Geeves MA (1995) Characterization of the equilibrium between blocked and closed states of muscle thin filaments. *Eur J Biochem* 227: 694–699.
17. Hidalgo C, Craig R, Ikebe M & Padrón R (2001) Mechanism of phosphorylation of the regulatory light chain of myosin from tarantula striated muscle. *Journal of Muscle Research and Cell Motility* 22: 51-59.
18. Hidalgo C, Wu Y, Peng J, Siems WF, Campbell KB, & Granzier H (2006) Effect of diastolic pressure on MLC2v phosphorylation in the rat left ventricle. *Arch Biochem Biophys.* 456:216-223.
19. Hofmann PA, Hartzell HC, & Moss RL. (1991) Alterations in Ca<sup>2+</sup> sensitive tension due to partial extraction of C protein from rat skinned cardiac myocytes and rabbit skeletal muscle fibers. *J Gen Physiol.* 97: 1141–1163
20. Hofmann PA & Fuchs F (1987b) Evidence for a force-dependent component of calcium binding to cardiac troponin C. *Am J Physiol* 253: C541–C546.
21. Holmes JW, Hunlich M, & Hasenfuss G (2002) Energetics of the Frank-Starling effect in rabbit myocardium: economy and efficiency depend on muscle length. *Am J Physiol Heart Circ Physiol* 283: H324-H330.
22. Huang, W et al. (2008) Myosin Regulatory Light Chain Phosphorylation Attenuates Cardiac Hypertrophy. *J. Biol. Chem.* 283: 19748-19756.
23. Janssen, PML et al. (1999) Preservation of Contractile Characteristics of Human Myocardium in Multi-day Cell Culture. *J Mol Cell Cardiol* 31, 1419–1427.
24. Janssen PML, Lehnart JP, Prestle J, Lynker JC, Just H, & Hasenfuss G (1998) The trabecula culture system: a novel technique to study contractile parameters over a multiday time period. *AM J Physiol Heart Circ Physiol* 274:1481-1488.
25. Julian FJ, & Sollins MR (1975) Sarcomere length-tension relations in living rat papillary muscle. *Circ. Res.* 1975;37;299-308.
26. Kajiwaraa H et al. (2000) Effect of Troponin I Phosphorylation by Protein Kinase A on Length-Dependence of Tension Activation in Skinned Cardiac Muscle Fibers. *Biochemical and Biophysical Research Communications* 272 (1): 104-110.

27. Kawai M, Wray JS & Zhao Y (1993) The effect of lattice spacing change on cross-bridge kinetics in chemically skinned rabbit psoas muscle fibers. I. proportionality between the lattice spacing and the fiber width. *Biophys J* 64: 187–196.
28. Kerrick WG et al. (2009) Malignant familial hypertrophic cardiomyopathy D166V mutation in the ventricular myosin regulatory light chain causes profound effects in skinned and intact papillary muscle fibers from transgenic mice. *FASEB J.* 23(3):855-865.
29. Kockskamper J, Lewinski D, Khafaga M, Elgner A, Grimm M, Eschenhagen T et al. (2008) The slow force response to stretch in atrial and ventricular myocardium from human heart: functional relevance and subcellular mechanisms. *Prog. Biophys. Mol. Biol.* 97 (2–3), 250–267.
30. Levine, RJ, Kensler RW, Yang Z, Stull JT, and Sweeney HL (1996) Myosin light chain phosphorylation affects the structure of rabbit skeletal muscle thick filaments. *Biophys. J.* 71:898–907.
31. Lakatta EG, & Jewell BR (1977) Length-dependent activation: Its effects on the length-tension relation in cat ventricular muscle. *Circ. Res.* 40;251-257.
32. Lorenzen-Schmidt I, et al. (2005) Young MLP deficient mice show diastolic dysfunction before the onset of dilated cardiomyopathy. *J Mol Cell Cardiol.* 39(2):241-50.
33. Marban E, Kusuoka H, Yue DT, Weisfeldt ML & Wier WG (1986) Maximal  $Ca^{2+}$ -activated force elicited by tetanization of ferret papillary muscle intact myocardium and whole heart: mechanism and characteristics of steady contractile activation in intact myocardium. *Circ. Res.* 59;262-269.
34. Marino TA, Houser SR, Martin FG & Freeman AR (1983) An ultrastructural morphometric study of the papillary muscle of the right ventricle of the cat. *Cell Tissue Res* 230, 543-552.
35. Martyn DA & Gordon AM (2001) Influence of length or force on activation-dependent changes in troponin C structure in skinned cardiac and fast skeletal muscle. *Biophys J* 80: 2798–2808.
36. McKillop DF, & Geeves MA (1993) Regulation of the interaction between actin and myosin subfragment 1: evidence for three states of the thin filament, *Biophys. J.* 65, 693–701.
37. Metzger, JM, Greaser ML, & Moss RL (1989) Variations in cross-bridge attachment rate and tension with phosphorylation of myosin in mammalian skinned skeletal muscle fibers. Implications for twitch potentiation in intact muscle. *J. Gen. Physiol.* 93:855–883.

38. Montgomery, DE et al. (2005) Protein kinase C induces systolic cardiac failure marked by exhausted inotropic reserve and intact Frank-Starling mechanism. *Am J Physiol Heart Circ Physiol* 289: H1881-H1888.
39. Morano I, et al. (1985) The influence of P-light chain phosphorylation by myosin light chain kinase on the calcium sensitivity of chemically skinned heart fibers. *FEBS Lett.* 23; 189(2): 221-224.
40. Moss RL (1992) Ca<sup>2+</sup> regulation of mechanical properties of striated muscle. Mechanistic studies using extraction and replacement of regulatory proteins. *Circ. Res.* 70; 865-884.
41. Olsson MC, Patel JR, Fitzsimons DP, Walker JW, & Moss RL (2004) Basal myosin light chain phosphorylation is a determinant of Ca<sup>2+</sup> sensitivity of force and activation dependence of the kinetics of myocardial force development. *Am J Physiol Heart Circ Physiol.* 287: H2712-8.
42. Pi, Y, Zhang D, Kemnitz KR, Wang H, & Walker JW (2003) Protein kinase C and A sites on troponin I regulate myofilament Ca<sup>2+</sup> sensitivity and ATPase activity in the mouse myocardium. *J. Physiol.* 552:845–857.
43. Pringle, J.W. 1978. The Croonian Lecture, 1977. Stretch activation of muscle: function and mechanism. *Proc. R. Soc. Lond. B. Biol. Sci.* 201:107–130.
44. Raskin AM, Masahiko H, Swanson E, McCulloch AD, & Omens JH (2009) Hypertrophic Gene Expression Induced by Chronic Stretch of Mouse Heart Muscle. *MCB* 124:1-15.
45. Redel A, Baumgartner W, Golenhofen K, Drenckhahn D & Golenhofen N (2002) Mechanical activity and force-frequency relationship of isolated mouse papillary muscle: Effects of extracellular calcium concentration, temperature and contraction type. *Pflugers. Arch* 445, 297-304.
46. Regnier M, Rivera AJ, Wang C-K, Bates MA, Chase PB & Gordon AM (2002) Thin filament near-neighbor regulatory unit interactions affect rabbit skeletal muscle steady-state force-Ca<sup>2+</sup> relations. *J Physiol* 540: 485–497.
47. Rossmann GH, Hoh JFY, Turnbull L, & Ludowyke RI. (1997) Mechanism of action of endothelin in rat cardiac muscle: cross-bridge kinetics and myosin light chain phosphorylation. *J Physiol* 505: 217–227.
48. Sanbe Dagger, A et al. (1999) Abnormal Cardiac Structure and Function in Mice Expressing Nonphosphorylatable Cardiac Regulatory Myosin Light Chain 2. *J Biol Chem* 274:30 ; 21085-21094.

49. Sarin V, Gaffin RD, Meininger GA & Muthuchamy M (2005) Arginine-glycine-aspartic acid (RGD)-containing peptides inhibit the force production of mouse papillary muscle bundles via alpha 5 beta 1 integrin. *J Physiol* 564, 603-617.
50. Scruggs SB, et al. (2009) Ablation of Ventricular Myosin Regulatory Light Chain Phosphorylation in Mice Causes Cardiac Dysfunction in Situ and Affects Neighboring Myofilament Protein Phosphorylation. *J. Biol. Chem.* 284, 8, 5097-5106.
51. Solaro JR. (2008) Multiplex Kinase Signaling Modifies Cardiac Function at the Level of Sarcomeric Proteins. *J. Biol. Chem.* 283(40): 26829-26833.
52. Steiger G.J. (1977) Tension transients in extracted rabbit heart muscle preparations. *J. Mol. Cell. Cardiol.* 9:671-685.
53. Stegmann H, Wepf R, Schröder RR, & Fink RH. (1999) Quantification of total calcium in terminal cisternae of skinned muscle fibers by imaging electron energy-loss spectroscopy. *Journal of Muscle Research and Cell Motility* 20: 505-515.
54. Stelzer JE, Dunning SB, & Moss RL (2006) Ablation of Cardiac Myosin-Binding Protein-C Accelerates Stretch Activation in Murine Skinned Myocardium. *Circulation Research.* 98:1212-1218
55. Stelzer JE, Patel JR, & Moss RL (2006) Acceleration of stretch activation in murine myocardium due to phosphorylation of myosin regulatory light chain. *J Gen Physiol.* 128:261-272.
56. Stull LB, Leppo M, Marban E, Janssen PML. Physiological determinants of contractile force generation and calcium handling in mouse myocardium. *J Mol Cell Cardiol* 2002; 34(xx):1367-1376.
57. Stuyvers BD, McCulloch AD, Guo J, Duff HJ & ter Keurs HE (2002) Effect of stimulation rate, sarcomere length and  $Ca^{2+}$  on force generation by mouse cardiac muscle. *J Physiol* 544, 817-830.
58. Sweeney HL & Stull JT (1986) Phosphorylation of myosin in permeabilized mammalian cardiac and skeletal muscle cells. *Am J Physiol Cell Physiol* 250: C657-C660.
59. Sweeney, HL, & Stull JT. (1990) Alteration in cross-bridge kinetics by myosin light chain phosphorylation in rabbit skeletal muscle: implications for regulation of actin-myosin interactions. *Proc. Natl. Acad. Sci. USA.* 87:414-418.

60. Szczesna D, Ghosh D, Li Q, et al. (2001) Familial hypertrophic cardiomyopathy mutations in the regulatory light chains of myosin affect their structure, Ca<sup>2+</sup> binding, and phosphorylation. *J Biol Chem.* 276:7086-7092.
61. Szczesna-Cordary D, Guzman G, Ng SS, & Zhaoriginally J (2004) Familial Hypertrophic Cardiomyopathy-linked Alterations in Ca<sup>2+</sup> Binding of Human Cardiac Myosin Regulatory Light Chain Affect Cardiac Muscle Contraction. *J. Biol. Chem.* 279 (5): 3535-3542.
62. Vemuri R, Lankford EB, Poetter K, Hassanzadeh S, Takeda K, Yu ZX, Ferrans VJ, & Epstein ND (1999) The stretch-activation response may be critical to the proper functioning of the mammalian heart. *Proc. Natl. Acad. Sci. USA.* 96:1048–1053.
63. Wamel, JET et al. (2000) Rapid gene transcription induced by stretch in cardiac myocytes and fibroblasts and their paracrine influence on stationary myocytes and fibroblasts. *Springer-Verlag Pflügers Arch* 439:781–788.
64. Wang H, Grant JE, Doede CM, Sadayappan S, Robbins J, & Walker, JW (2006) PKC-βII sensitizes cardiac myofilaments to Ca<sup>2+</sup> by phosphorylating troponin I on threonine-144. *J. Mol. Cell. Cardiol.* 41, 823–833.
65. Wang Y-P and Fuchs F (1994) Length, force, and Ca<sup>2+</sup>-troponin C affinity in cardiac and slow skeletal muscle. *Am J Physiol* 266: C1077–C1082.
66. Yang Z, Stull JT, Levine RJC and Sweeney HL (1998) Changes in interfilament spacing mimic the effects of myosin regulatory light chain phosphorylation in rabbit psoas fibers. *J Struct Biol* 122:139–148.